Cell Stress and Chaperones (2023) 28:177–190
https://doi.org/10.1007/s12192-023-01328-x

ORIGINAL ARTICLE

CircHSPG2 knockdown attenuates hypoxia-induced apoptosis, inflammation, and oxidative stress in human AC16 cardiomyocytes by regulating the miR-1184/MAP3K2 axis

Liu Huang[1] · Bingyan Guo[1] · Jie Yan[1] · Huiqing Wei[1] · Suyun Liu[1] · Yongjun Li[1]

Received: 22 November 2022 / Revised: 2 February 2023 / Accepted: 3 February 2023 / Published online: 21 February 2023

Abstract

Circular RNAs (circRNAs) have been identified as vital regulators in cardiovascular diseases, including acute myocardial infarction (AMI). In this study, the function and mechanism of circRNA heparan sulfate proteoglycan 2 (circHSPG2) in hypoxia-induced injury in AC16 cardiomyocytes were investigated. AC16 cells were stimulated with hypoxia to establish an AMI cell model in vitro. Real-time quantitative PCR and western blot assays were performed to quantify the expression levels of circHSPG2, microRNA-1184 (miR-1184), and mitogen-activated protein kinase kinase kinase 2 (MAP3K2). Counting Kit-8 (CCK-8) assay was used to measure cell viability. Flow cytometry was performed to detect cell cycle and apoptosis. Enzyme-linked immunosorbent assay (ELISA) was used to determine the expression of inflammatory factors. Dual-luciferase reporter, RNA immunoprecipitation (RIP), and RNA pull-down assays were used to analyze the relationship between miR-1184 and circHSPG2 or MAP3K2. In AMI serum, circHSPG2 and MAP3K2 mRNA were highly expressed and miR-1184 was down-regulated. Hypoxia treatment elevated HIF1α expression and repressed cell growth and glycolysis. Moreover, hypoxia promoted cell apoptosis, inflammation, and oxidative stress in AC16 cells. Hypoxia-induced circHSPG2 expression in AC16 cells. CircHSPG2 knockdown alleviated hypoxia-induced AC16 cell injury. CircHSPG2 directly targeted miR-1184, and miR-1184 targeted and suppressed MAP3K2. Inhibition of miR-1184 or overexpression of MAP3K2 abolished the alleviated effect of circHSPG2 knockdown on hypoxia-induced AC16 cell injury. Overexpression of miR-1184 relieved hypoxia-induced impairment in AC16 cells by MAP3K2. CircHSPG2 could regulate MAP3K2 expression through miR-1184. CircHSPG2 knockdown protected AC16 cells from hypoxia-induced injury by regulating the miR-1184/MAP3K2 cascade.

Keywords AMI · Hypoxia · circHSPG2 · miR-1184 · MAP3K2 · Cardiomyocytes

Introduction

Acute myocardial infarction (AMI) is a fatal cardiovascular disease worldwide (Boateng and Sanborn 2013). AMI is associated with acute ischemia-hypoxia-induced dysfunction in cardiomyocytes, ultimately leading to irreversible myocardial damage (Gong et al. 2021; Lu et al. 2015). AMI can induce cardiomyocyte apoptosis, oxidative stress, and inflammatory response, thereby leading to cardiomyocyte injury (Del Re et al. 2019; Ye et al. 2014). Therefore, revealing the mechanism of hypoxia-induced cardiomyocyte dysfunction is crucial for understanding the pathogenesis of AMI and developing new therapeutic targets.

Circular RNAs (circRNAs) are naturally occurring RNA circles with a closed continuous loop structure (Memczak et al. 2013). CircRNAs exert their functions in biological processes by acting as sponges for microRNAs (miRNAs), functionally liberating mRNA transcripts targeted by that set of miRNAs (Panda 2018; Fabian et al. 2010). Many circRNAs are linked to the pathogenesis of cardiovascular diseases, including AMI (Sun et al. 2020; Zhao et al. 2020). As an example, circ_0060745 silencing ameliorated cardiomyocyte apoptosis and inflammation under hypoxia conditions by inactivating the NF-κB pathway (Zhai et al. 2020). Circ_0023461 aggravated hypoxia-caused dysfunction in cardiomyocytes by enhancing PDE4D expression through miR-370-3p (Ren et al.

✉ Yongjun Li
lyjbs2018@126.com

[1] Department of Cardiovascular Medicine, The Second Hospital of Hebei Medical University, No. 215 Heping West Road, Shijiazhuang 050000, China

2021). CircRNA heparan sulfate proteoglycan 2 (circHSPG2, also named hsa_circ_0010551) is overexpressed in AMI as shown by microarray gene chip analysis (Yin et al. 2021). However, it is still unclear whether abnormal expression of circHSPG2 is related to AMI pathogenesis.

MiRNAs are involved in multiple biological processes (Liu et al. 2014). Dysregulation of miRNAs plays a vital role in the development of AMI by influencing cardiomyocyte apoptosis and inflammation (Yan et al. 2017). Aberrant expression of miR-1184 is related to the pathogenesis of various diseases, such as sepsis (Ling et al. 2021), colorectal cancer (Wang et al. 2020), and bladder cancer (Yang et al. 2020). Moreover, miR-1184 can promote cell viability and repress the apoptosis in mouse cardiomyocytes through the circROBO2/miR-1184/TRADD regulatory cascade (Chen et al. 2021). Nonetheless, whether circHSPG2 can target miR-1184 is unknown currently.

In this study, we explored the function and mechanism of circHSPG2 in AMI pathogenesis using a hypoxia-induced AMI cell model in vitro, with the hope that such a study might discover novel targets for AMI treatment.

Materials and methods

Human serum collection

A total of 37 AMI patients and 37 healthy volunteers at the First Affiliated Hospital of Hainan Medical University were enrolled in this study. The basic clinical information of all participants is shown in Table 1. Blood specimens were collected from these participants, and serum samples were obtained to quantify the expression of circHSPG2, miR-1184, and mitogen-activated protein kinase kinase kinase 2 (MAP3K2). All participants signed written informed consent, and the Ethics Committee of the Second Hospital of Hebei Medical University approved the study.

Table 1 The basic clinical information of healthy volunteers and AMI patients

Characteristics	Healthy volunteers ($n=37$)	AMI patients ($n=37$)
Gender (female:male)	19:18	12:25
Age (years)	52.4 ± 12.1	59.6 ± 11.4
BMI	23.6 ± 2.1	26.5 ± 3.2
Smoke (n, %)	16, 43.2%	27, 73.0%
Alcohol (n, %)	20, 54.1%	29, 78.4%

Cell culture and hypoxia treatment

Human AC16 cardiomyocytes (BeNa Culture Collection, Beijing, China) were cultured in DMEM (Invitrogen, Carlsbad, CA, USA) supplemented with 10% FBS (Invitrogen) and 1% penicillin–streptomycin (Invitrogen) at 37 °C in an incubator containing 5% CO_2. For hypoxia treatment, AC16 cells were cultured in a hypoxic incubator (5% CO_2, 1% O_2, and 94% N_2) for 0 h, 12 h, 24 h, and 48 h. As the normoxia control, cells were cultured in the normoxia incubator (5% CO_2, 21% O_2, and 74% N_2). To establish the in vitro hypoxia-induced cardiomyocyte injury model, AC16 cells were cultured for 24 h under hypoxia conditions.

Cell transfection

CircHSPG2 small interfering RNAs (si-circHSPG2#1, 5′-TGGTCACTGTCACCCACACCC-3′ and si-circHSPG2#2, 5′-TCACTGTCACCCACACCCTGC-3′), control siRNA (si-NC, 5′-TCGACTCAGACTCGCTCTCGC-3′), the mimic and inhibitor of miR-1184 (miR-1184 and in-miR-1184), negative controls miR-NC and in-miR-NC, MAP3K2 overexpression vector (MAP3K2) and empty vector control were synthesized by GenePharma (Shanghai, China). Then, the synthetic oligonucleotides or/and vectors were transfected into AC16 cells using Lipofectamine 2000 (Invitrogen). After 48 h of transfection, the cells were harvested for further experiments or subjected to hypoxia treatment as above.

Real-time quantitative PCR

RNA was extracted from serum samples and cells (1×10^7) using TRIzol reagent and protocols (Invitrogen). The reverse transcription (RT) experiment was conducted with M-MLV RT Reagent (Promega, Madison, WI, USA; for mRNA and circRNA analyses) or miRNA 1st Strand cDNA Synthesis Reagent (Vazyme, Nanjing, China; for miRNA analysis). RNA expression levels were quantified by real-time quantitative PCR with SYBR Green qPCR Mix (Vazyme). The results were analyzed by the $2^{-\Delta\Delta Ct}$ method and normalized to β-actin or U6. The primers are exhibited in Table 2.

Cell counting kit-8 (CCK-8) assay

Using CCK-8 assay reagent (Beyotime, Shanghai, China), AC16 cell viability was determined. In brief, AC16 cells after the indicated treatment or/and transfection were seeded into 96-well plates at 4×10^3 cells/well and cultured for 48 h. Then, CCK-8 reagent was added into each well and

Table 2 Primers sequences used for qRT-PCR

Name		Primers for PCR (5′-3′)
CircHSPG2	Forward	CAGGGTGTGGGTGACAGTG
	Reverse	ACCGTCAGGAATGCCAAACA
HSPG2	Forward	TCTCATCCCAGGGTGACAGT
	Reverse	GTAGAAGTGGCCGTCAGGG
miR-1184	Forward	GCCGAGCCTGCAGCGACTTGATG
	Reverse	CTCAACTGGTGTCGTGGAG
MAP3K2	Forward	AAACAACGACCAGGACGCTC
	Reverse	TCGCTAGAGACCGGAGAAGA
β-actin	Forward	TGGATCAGCAAGCAGGAGTA
	Reverse	TCGGCCACATTGTGAACTTT
U6	Forward	CTCGCTTCGGCAGCACA
	Reverse	AACGCTTCACGAATTTGCGT

incubation was performed at 37 °C for 2 h. The optical density value at 450 nm was detected using a microplate reader (Bio-Rad, Hercules, CA, USA).

RNase R and actinomycin D assays

For RNase R treatment, 1 μg RNA of AC16 cells was treated with or without RNase R (Epicenter Biotechnologies, Madison, WI, USA) and then subjected to real-time quantitative PCR for the quantification of circHSPG2 and linear HSPG2 levels. For the Actinomycin D assay, AC16 cells were exposed to Actinomycin D (Sigma-Aldrich, St. Louis, MO, USA) for the indicated time points. Then, the expression levels of circHSPG2 and linear HSPG2 mRNA were evaluated by real-time quantitative PCR.

Subcellular fraction analysis

To determine the cellular localization of circHSPG2, the Cytoplasmic and Nuclear RNA Purification reagent (Norgen Biotek, Thorold, ON, Canada) was utilized according to the manufacturer's protocols. The expression levels of circHSPG2 in the nucleus fraction and cytoplasm fraction were determined by real-time quantitative PCR.

Flow cytometry

The Annexin V-fluorescein isothiocyanate (FITC)/propidium iodide (PI) Detection Kit (Vazyme) was employed to detect cell cycle progression and cell apoptosis. For cell cycle detection, treated AC16 cells (1×10^6) were washed with PBS and fixed with 75% ethanol. Next, the cells were re-suspended and dyed with PI for 15 min in the dark. For cell apoptosis detection, AC16 cells (5×10^6) were collected, re-suspended, and stained with Annexin V-FITC and PI for 15 min. Then, cell cycle distribution and cell apoptosis were estimated using flow cytometry (FACS Canto II flow cytometer, BD Biosciences, San Jose, CA, USA) and Cell-Quest software. PI signals were detected via a 585/42 nm band pass filter, and FITC signals were detected via a 530/30 nm band pass filter. The apoptotic rate was determined by calculating the sum of the percentage of early (Annexin V^+/PI^-) and late (Annexin V^+/PI^+) apoptotic cells.

Western blot assay

Total protein was extracted from cultured AC16 cells (1×10^7) with RIPA buffer (Beyotime). Protein samples were separated by 10% SDS-PAGE gels and then blotted onto PVDF membranes (Millipore, Shanghai, China). The membranes were blocked with 5% non-fat milk and then probed with related primary antibodies, followed by the incubation with the secondary antibody. The bands were visualized by ECL reagent (Beyotime). The primary antibodies against HIF1α (rabbit monoclonal, ab179483, 1:1000), IL-6 (rabbit monoclonal, ab233706, 1:1000), TNF-α (rabbit monoclonal, ab183218, 1:2000), B-cell lymphoma-2 (Bcl-2; rabbit monoclonal, ab182858, 1:2000), BCL2-Associated X (Bax; rabbit monoclonal, ab32503, 1:3000), cleaved caspase 3 (rabbit polyclonal, ab2302, 1:100), MAP3K2 (rabbit monoclonal, ab33918, 1:10,000), and β-actin (rabbit polyclonal, ab8227, 1:3000) and the goat anti-rabbit IgG secondary antibody conjugated by HRP (ab6721, 1:5000) were purchased from Abcam (Cambridge, UK).

Enzyme-linked immunosorbent assay (ELISA)

The production levels of interleukin-6 (IL-6) and tumor necrosis factor α (TNF-α) in the supernatant of treated AC16 cells were determined by ELISA using IL-6 (ab178013) and TNF-α (ab181421) ELISA kits (both from Abcam), respectively, following the manufacturer's instructions.

Measurement of malonaldehyde (MDA) and superoxide dismutase (SOD)

MDA level and SOD activity in treated AC16 cells were examined with the MDA assay kit and SOD assay kit (both from Sigma-Aldrich), respectively, based on the manufacturer's instructions.

Detection of glucose uptake and lactate production

The glycolysis level of treated AC16 cells was evaluated by determining glucose uptake level and lactate production with glucose and lactate assay kits (Sigma-Aldrich), respectively, according to the manufacturer's protocols.

Dual-luciferase reporter assay

The fragments of circHSPG2 and MAP3K2 3'UTR harboring the wild-type (WT) or mutant (MUT) binding sites of miR-1184 were subcloned into the pmirGLO vector (Promega) to produce circHSPG2 WT, circHSPG2 MUT, MAP3K2 3′UTR WT, and MAP3K2 3′UTR MUT. AC16 cells (1×10^6) were introduced with the reporter constructs and miR-1184 mimic or miR-NC mock. After 48 h, the luciferase intensity was measured using the Dual-Luciferase Reporter Assay kit (Promega).

RNA immunoprecipitation (RIP) assay

The Magna RIP™ RNA Binding Protein Immunoprecipitation Kit (Millipore, Bedford, MA, USA) was used to analyze the relationship between circHSPG2 and miR-1184. AC16 cells (5×10^6) were lysed in RIPA buffer and then incubated with magnetic beads conjugated with the anti-AGO2 or anti-IgG antibody. RNA was extracted from the beads and processed by real-time quantitative PCR for the quantification of the enrichment levels of circHSPG2 and miR-1184.

RNA pull-down assay

The biotin-labeled probes of wild-type miR-1184 (Bio-miR-1184 WT), mutant miR-1184 (Bio-miR-1184 MUT), and negative Bio-NC were synthesized by GenePharma. Lysates of AC16 cells (5×10^6) were incubated with streptavidin magnetic beads (Invitrogen) conjugated with the probes. RNA was extracted from the beads and subjected to real-time quantitative PCR for the evaluation of the circHSPG2 enrichment level.

Statistical analysis

All experiments were repeated three times, and all data were analyzed with GraphPad Prism 7. The differences in the two groups were analyzed by an unpaired Student's *t*-test, and multiple groups were compared by one-way ANOVA with Tukey's post hoc test. The results were exhibited as mean ± SD. Differences with *P* values of < 0.05 were considered significant. The experimental timeline under hypoxia conditions is shown in Supplementary Fig. 1.

Results

Hypoxia treatment repressed cell viability and increased HIF1α level in AC16 cells

AC16 cells were exposed to hypoxia for 0 h, 12 h, 24 h, and 48 h, and then a CCK-8 assay was conducted to determine cell viability. The results showed that hypoxia treatment suppressed the viability of AC16 cells (Fig. 1A). HIF1α is an indicator of hypoxia, and we then determined its expression in AC16 cells after hypoxia treatment. The results of real-time quantitative PCR and western blot showed that hypoxia treatment elevated HIF1α expression at both mRNA and protein in AC16 cells (Fig. 1B and C).

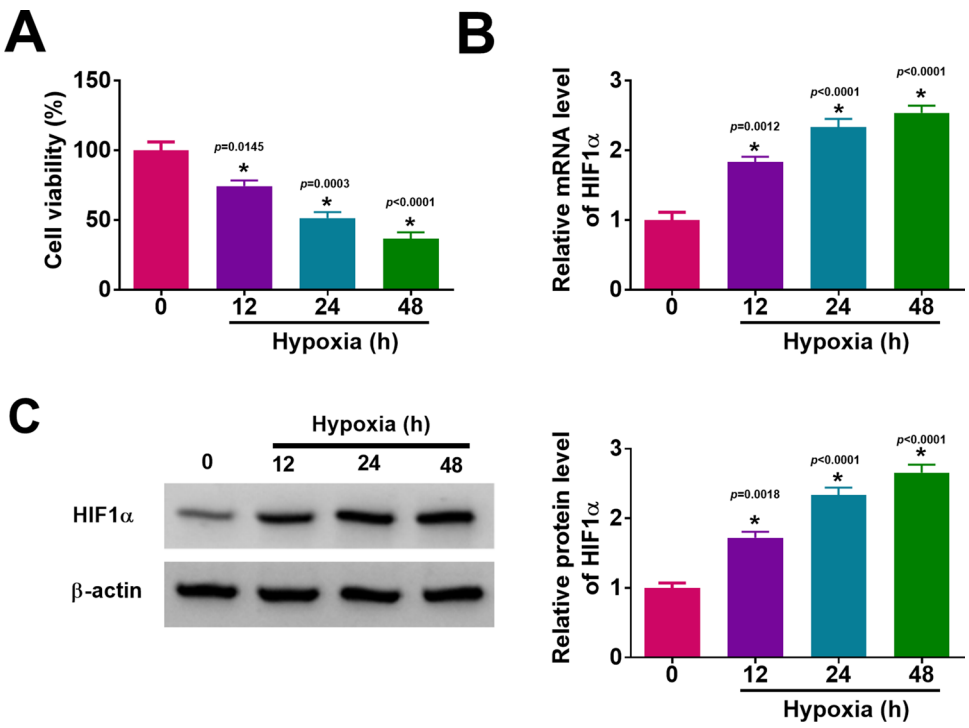

Fig. 1 Cell viability was repressed and HIF1α level was increased in hypoxia-treated AC16 cells. **A** The viability of AC16 cells treated with hypoxia for 0 h, 12 h, 24 h, and 48 h was examined by CCK-8 assay. **B** and **C** The mRNA and protein levels of HIF1α in AC16 cells treated with hypoxia for 0 h, 12 h, 24 h, and 48 h were measured by real-time quantitative PCR and western blot. $^*P < 0.05$

CircHSPG2 level was upregulated in AMI serum and hypoxia-induced AC16 cells

The expression levels of circHSPG2 in the serum samples of AMI patients and healthy controls were determined by real-time quantitative PCR. The results showed that circHSPG2 was overexpressed in AMI patients compared to healthy controls (Fig. 2A). Moreover, circHSPG2 level in AC16 cells was increased by hypoxia treatment for 24 h compared to the normoxia group (Fig. 2B). RNase R assays showed that circHSPG2 was resistant to RNase R digestion (Fig. 2C). After incubation with Actinomycin D, circHSPG2 level was not affected in AC16 cells (Fig. 2D). Whereas, the linear HSPG2 level was markedly reduced by RNase R digestion and actinomycin D incubation (data not shown). Moreover, subcellular fraction analysis showed that circHSPG2 was mainly enriched in the cytoplasm of AC16 cells (Fig. 2E). As illustrated in Fig. 2F, circHSPG2 is a circular transcript generated by back-splicing of exons 12–93 of HSPG2 pre-mRNA. These findings indicated that circHSPG2 was highly expressed in AMI.

CircHSPG2 knockdown attenuated the effects of hypoxia on cell viability, cell cycle progression, apoptosis, inflammation, oxidative stress, and glycolysis in AC16 cells

Next, the functional role of circHSPG2 in hypoxia-induced AC16 cell injury was investigated. Transfection of si-circHSPG2#1 or si-circHSPG2#2 (their sequences are shown in Fig. 2F), but not si-NC control, knocked down circHSPG2 expression (Fig. 3A). The upregulation of circHSPG2 in hypoxia-treated AC16 cells was reversed by transfection of si-circHSPG2#1 or si-circHSPG2#2 (Fig. 3B). CCK-8 assays showed that hypoxia treatment repressed AC16 cell viability, while circHSPG2 knockdown reversed the effect (Fig. 3C). Flow cytometry results indicated that in hypoxia-treated AC16 cells, cell cycle was arrested in G0/G1 phase, and cell apoptosis was facilitated; these effects were weakened by circHSPG2 silencing (Fig. 3D and E and Supplementary Fig. 2A). The levels of anti-apoptotic protein Bcl-2 and pro-apoptotic proteins Bax and cleaved caspase 3 in AC16 cells under hypoxia conditions were then measured.

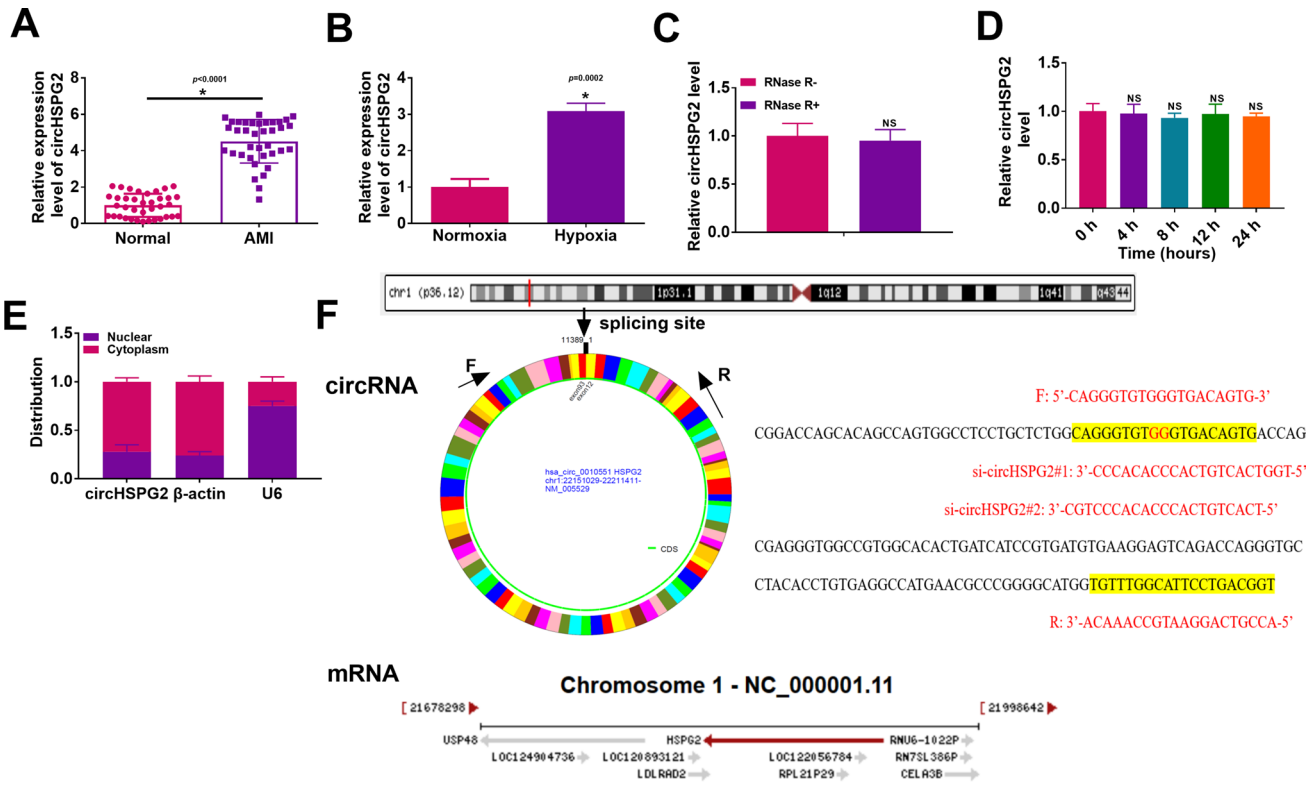

Fig. 2 High expression of circHSPG2 in AMI patients and hypoxia-treated AC16 cells. **A** The expression of circHSPG2 in the serum samples of AMI patients and healthy controls was determined by real-time quantitative PCR. **B** The expression of circHSPG2 in hypoxia-induced AC16 cells was determined by real-time quantitative PCR. **C** After RNase R treatment, circHSPG2 level in AC16 cells was detected by real-time quantitative PCR. **D** The expression of circHSPG2 in AC16 cells treated with Actinomycin D for 0 h, 4 h, 8 h, 12 h, and 24 h was detected by real-time quantitative PCR. **E** The distribution of circHSPG2 in the nucleus and cytoplasm of AC16 cells was examined through subcellular fraction analysis. **F** Schematic of the circular structure of circHSPG2 and the sequences of divergent primers, si-circHSPG2#1 and si-circHSPG2#2. $^{*}P < 0.05$

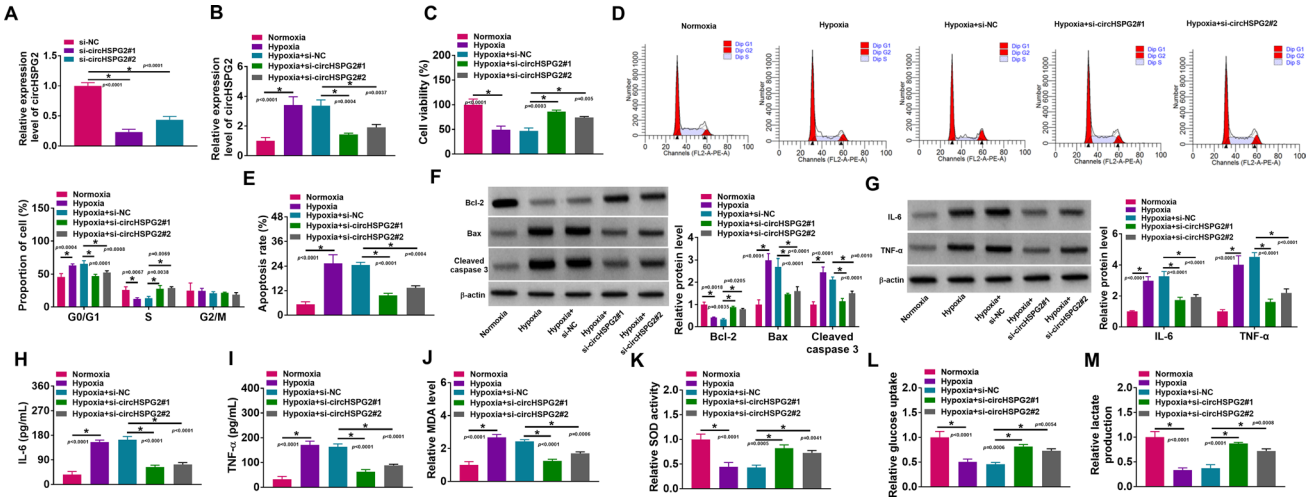

Fig. 3 CircHSPG2 knockdown promoted cell growth and glycolysis and inhibited apoptosis, inflammation, and oxidative stress in hypoxia-induced AC16 cells. **A** The expression of circHSPG2 in AC16 cells transfected with si-NC, si-circHSPG2#1, or si-circHSPG2#2. **B**–**M** AC16 cells were treated with normoxia, hypoxia, hypoxia + si-NC, hypoxia + si-circHSPG2#1, or hypoxia + si-circHSPG2#2. **B** The expression of circHSPG2 in AC16 cells was determined by real-time quantitative PCR. **C** AC16 cell viability was assessed by CCK-8 assay. **D** and **E** The cell cycle distribution and apoptosis of AC16 cells were analyzed by flow cytometry analysis. **F** The protein levels of Bcl-2, Bax, and cleaved caspase-3 in AC16 cells were measured by western blot. **G**–**I** The levels of IL-6 and TNF-α in AC16 cells were examined by ELISA and western blot. **J** and **K** MDA level and SOD activity were examined with the commercial kits. **L** and **M** The levels of glucose uptake and lactate production in AC16 cells were detected by the commercial kits. $*P < 0.05$

The results exhibited that hypoxia treatment decreased Bcl-2 levels and increased Bax and cleaved caspase 3 levels, while circHSPG2 interference ameliorated these effects (Fig. 3F). Our results also showed that hypoxia treatment increased the production levels of IL-6 and TNF-α in AC16 cells, while circHSPG2 silencing abated the impact (Fig. 3G–I). Then, oxidative stress in hypoxia-induced AC16 cells was evaluated by determining MDA level and SOD activity. Hypoxia treatment led to augmentation of MDA level and suppression of SOD activity in AC16 cells, while these effects were ameliorated by silencing of circHSPG2 (Fig. 3J and K). Additionally, hypoxia treatment inhibited glucose uptake and lactate production in AC16 cells, whereas circHSPG2 deficiency abated the effects (Fig. 3L and M). All these results suggested that circHSPG2 knockdown alleviated hypoxia-induced injury in AC16 cells.

CircHSPG2 directly targeted miR-1184 to regulate miR-1184 expression

To explore the underlying mechanism by which circHSPG2 silencing attenuated hypoxia-induced AC16 cell injury, circinteractome software (https://circinteractome.nia.nih.gov/) was utilized to search the potential target miRNAs of circHSPG2. The predicted data found that miR-1184 contained the putative binding sites of crcHSPG2 (Fig. 4A). The transfection efficacy assays revealed that miR-1184 mimic transfection increased miR-1184 expression, and in-miR-1184 transfection resulted in decreased expression of miR-1184 in AC16 cells (Fig. 4B). Dual-luciferase reporter assays showed that miR-1184 overexpression repressed the luciferase activity of circHSPG2 WT, while it did not affect the luciferase activity of circHSPG2 MUT in AC16 cells (Fig. 4C). RIP assays showed that circHSPG2 and miR-1184 were significantly enriched in anti-AGO2 RIP complexes compared to anti-IgG controls (Fig. 4D). RNA pull-down assays showed that circHSPG2 was markedly pulled down by Bio-miR-1184 WT, and this effect was abrogated by Bio-miR-1184 MUT (Fig. 4E). These results demonstrated the direct interaction between circHSPG2 and miR-1184. Additionally, the miR-1184 level was decreased in the serum samples of AMI patients and hypoxia-treated AC16 cells (Fig. 4F and G). Furthermore, circHSPG2 knockdown led to an increase in miR-1184 expression in AC16 cells, while in-miR-1184 transfection abated the effect (Fig. 4H). Taken together, circHSPG2 directly targeted miR-1184.

CircHSPG2 knockdown alleviated hypoxia-induced AC16 cell injury by miR-1184

The relationship between circHSPG2 and miR-1184 in the regulation of hypoxia-induced AC16 cell injury was then explored. As exhibited in Fig. 5A, circHSPG2 knockdown increased miR-1184 expression in hypoxia-treated AC16 cells, while the effect was abolished by in-miR-1184 transfection. The results of CCK-8 assays showed that circHSPG2 depletion facilitated the viability of hypoxia-treated AC16 cells, while miR-1184 inhibition abrogated the effect

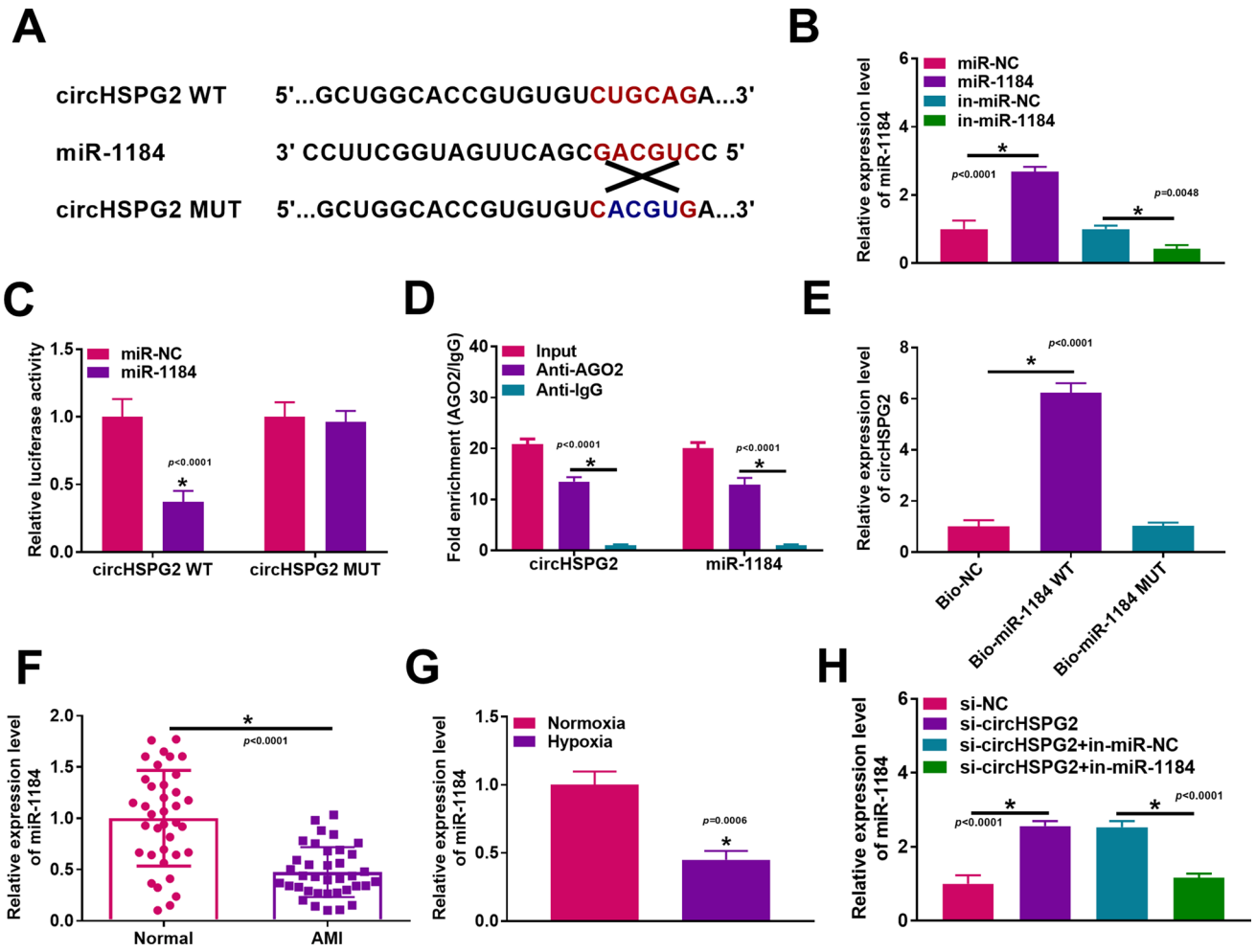

Fig. 4 MiR-1184 was targeted by circHSPG2. **A** The binding sites between circHSPG2 and miR-1184. **B** The expression of miR-1184 in AC16 cells transfected with miR-NC, miR-1184, in-miR-NC, or in-miR-1184 was determined by real-time quantitative PCR. **C**–**E** The combination between miR-1184 and circHSPG2 was verified by dual-luciferase reporter assay, RIP assay, and RNA pull-down assay. **F** and **G** The expression of miR-1184 in AMI patients and hypoxia-induced AC16 cells was determined by real-time quantitative PCR. **H** The expression of miR-1184 in AC16 cells transfected with si-NC, si-circHSPG2, si-circHSPG2 + in-miR-NC, or si-circHSPG2 + in-miR-1184 was detected by real-time quantitative PCR. $^*P < 0.05$

(Fig. 5B). Flow cytometry analysis showed that miR-1184 inhibition reversed the effects of circHSPG2 knockdown on cell cycle progression and apoptosis of hypoxia-treated AC16 cells (Fig. 5C and D and Supplementary Fig. 2B). Silencing of circHSPG2 increased Bcl-2 level and decreased Bax and cleaved caspase 3 levels in hypoxia-stimulated AC16 cells, whereas the effects were reversed by miR-1184 inhibition (Fig. 5E). Also, circHSPG2 interference declined the levels of IL-6 and TNF-α in AC16 cells under hypoxia conditions, while miR-1184 downregulation reversed the effects (Fig. 5F–H). CircHSPG2 knockdown-mediated effects on MDA level and SOD activity in hypoxia-treated AC16 cells were also ameliorated by the reduction of miR-1184 (Fig. 5I and J). Additionally, circHSPG2 knockdown promoted glucose uptake and lactate production in AC16 cells treated with hypoxia, while miR-1184 inhibition reversed the effects (Fig. 5K and L). Taken together, circHSPG2 silencing rescued hypoxia-induced AC16 cell damage by the upregulation of miR-1184.

MiR-1184 directly targeted and suppressed MAP3K2

Using targetscan program (http://www.targetscan.org/vert_71/), we found that MAP3K2 was a potential target of miR-1184 (Fig. 6A). Dual-luciferase reporter assays showed that miR-1184 mimic transfection markedly reduced the luciferase activity of MAP3K2 3'UTR WT, but not MAP3K2 3′UTR MUT, indicating the targeting of MAP3K2 by miR-1184 (Fig. 6B). MAP3K2 mRNA level was increased in the serum samples of AMI patients compared with normal controls (Fig. 6C). Moreover, the protein level of MAP3K2 was increased by hypoxia treatment in AC16 cells (Fig. 6D).

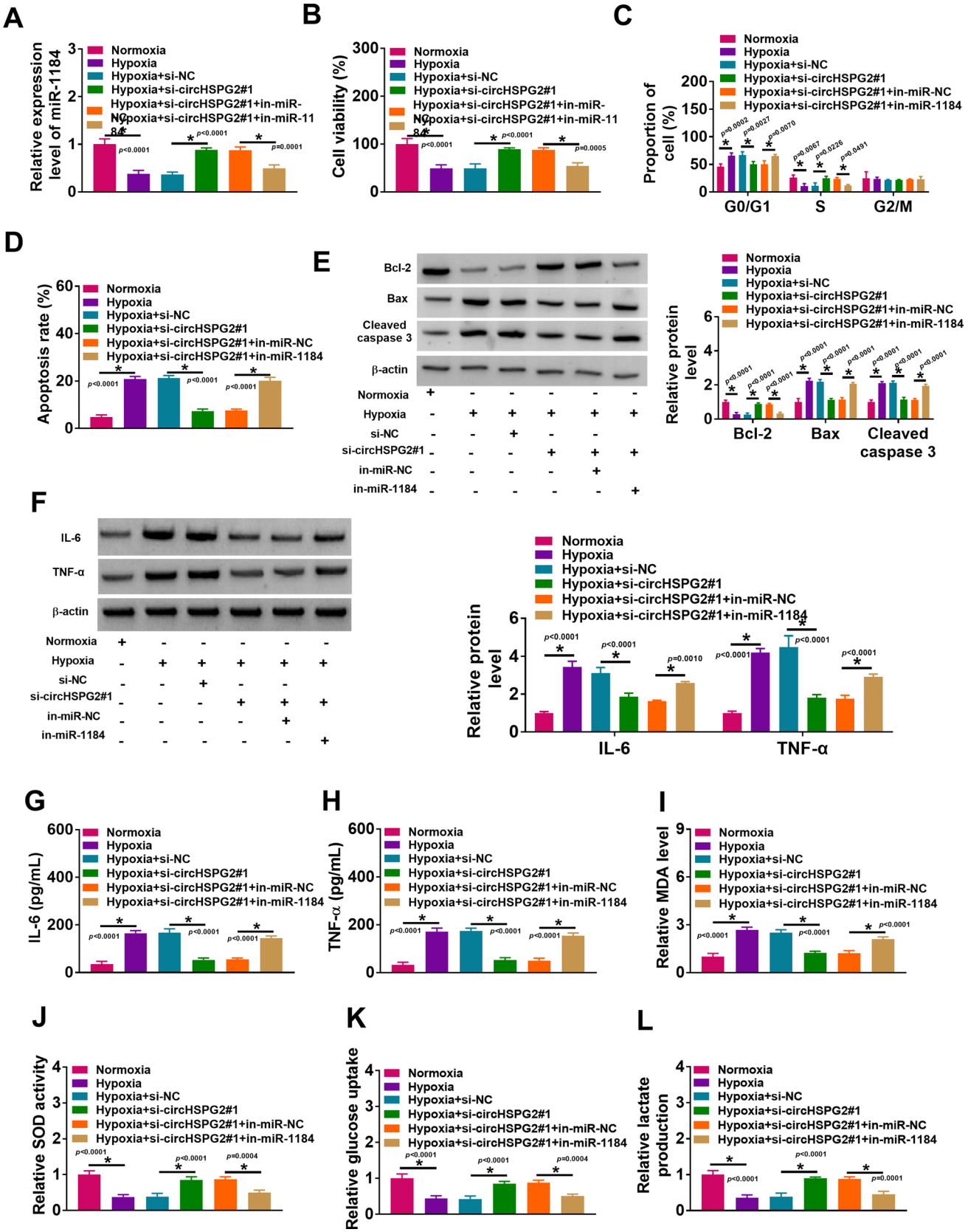
A
Relative expression level of miR-1184
Normoxia
Hypoxia
Hypoxia+si-NC
Hypoxia+si-circHSPG2#1
Hypoxia+si-circHSPG2#1+in-miR-NC
Hypoxia+si-circHSPG2#1+in-miR-11
B
Cell viability (%)
C
Proportion of cell (%)
G0/G1
S
G2/M
D
Apoptosis rate (%)
E
Bcl-2
Bax
Cleaved caspase 3
β-actin
Relative protein level
F
IL-6
TNF-α
G
IL-6 (pg/mL)
H
TNF-α (pg/mL)
I
Relative MDA level
J
Relative SOD activity
K
Relative glucose uptake
L
Relative lactate production

◂**Fig. 5** CircHSPG2 depletion regulated cell growth, cell apoptosis, inflammation, oxidative stress, and glycolysis in hypoxia-induced AC16 cells via miR-1184. AC16 cells were treated with normoxia, hypoxia, hypoxia + si-NC, hypoxia + si-circHSPG2, hypoxia + si-circHSPG2 + in-miR-NC, or hypoxia + si-circHSPG2 + in-miR-1184. **A** The expression of miR-1184 in AC16 cells was detected by real-time quantitative PCR. **B** AC16 cell viability was assessed by CCK-8 assay. **C** and **D** The cell cycle and cell apoptosis in AC16 cells were analyzed by flow cytometry analysis. **E** The protein levels of Bcl-2, Bac, and cleaved caspase 3 in AC16 cells were measured via western blot. **F**–**H** The concentrations of IL-6 and TNF-α in AC16 cells were examined with ELISA and western blot. **I** and **J** MDA level and SOD activity in AC16 cells were examined with the commercial kits. **K** and **L** The levels of glucose uptake and lactate production in AC16 cells were determined by the commercial kits. *$P < 0.05$

MiR-370-3p is downregulated in hypoxia-induced AC16 cells (Zhang et al. 2022; Ren et al. 2021), and bioinformatics data predict no targeted association between miR-370-3p and MAP3K2. Through a negative control miR-370-3p, we found that miR-1184 overexpression reduced MAP3K2 protein level in AC16 cells, while the effect was rescued by transfection of MAP3K2 overexpression vector (Fig. 6E). Additionally, circHSPG2 silencing markedly reduced MAP3K2 protein level in AC16 cells, while miR-1184 inhibition ameliorated the effect (Fig. 6F). Collectively, circHSPG2 positively regulated MAP3K2 expression by miR-1184.

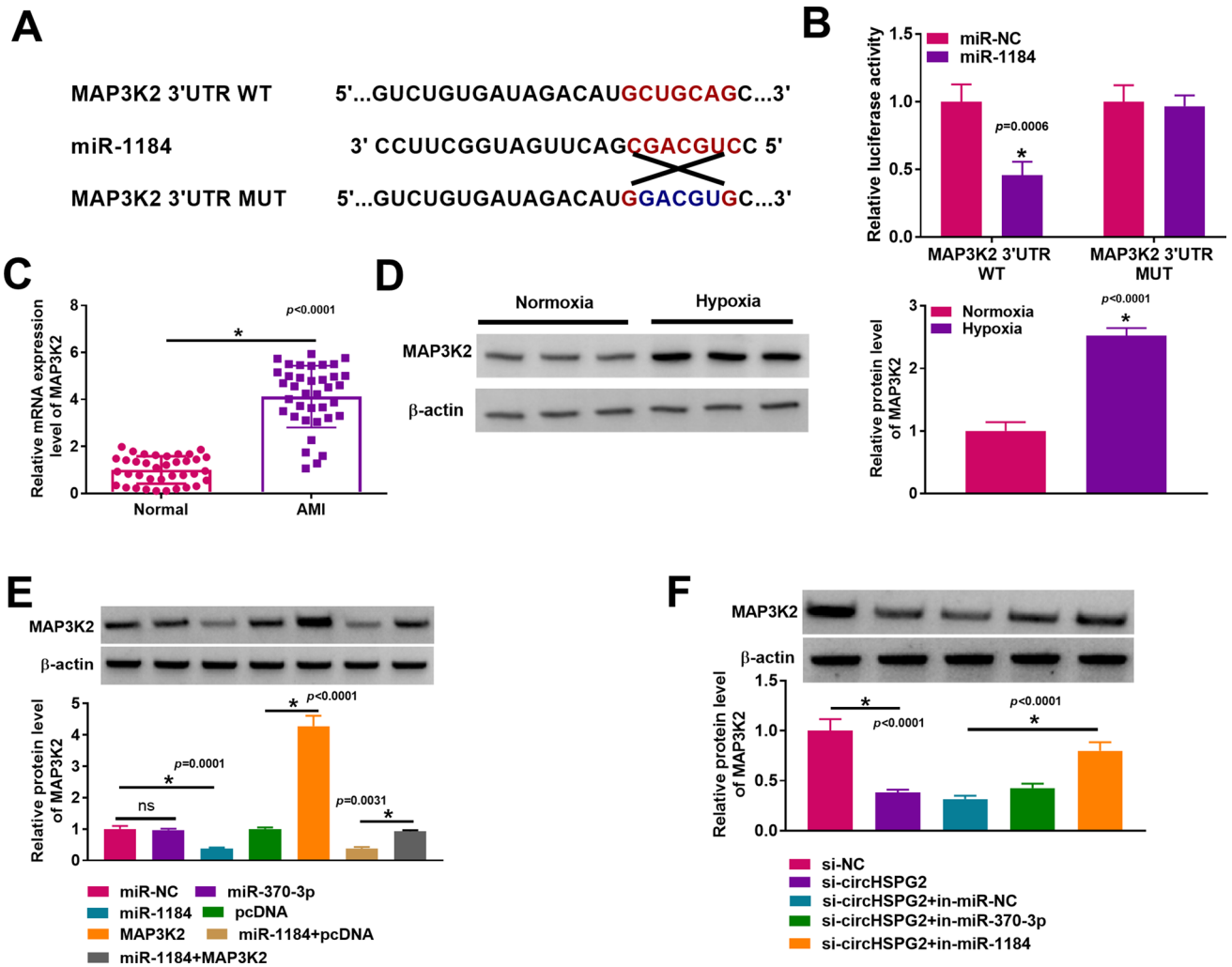

Fig. 6 MAP3K2 was a direct target of miR-1184. **A** The binding sites between miR-1184 and MAP3K2. **B** The interaction between miR-1184 and MAP3K2 was verified by dual-luciferase reporter assay. **C** The mRNA level of MAP3K2 in AMI patients and normal volunteers was determined by real-time quantitative PCR. **D** The protein level of MAP3K2 in AC16 cells under the normoxia or hypoxia condition was measured via western blot. **E** After AC16 cells were transfected with miR-NC mimic, miR-370-3p mimic, miR-1184 mimic, pcDNA, MAP3K2 overexpression plasmid, miR-1184 mimic + pcDNA, or miR-1184 mimic + MAP3K2 overexpression plasmid, the protein level of MAP3K2 in AC16 cells was measured via western blot. **F** The protein level of MAP3K2 in AC16 cells transfected with si-NC, si-circHSPG2, si-circHSPG2 + in-miR-NC, si-circHSPG2 + in-miR-370-3p, or si-circHSPG2 + in-miR-1184 was detected via western blot. *$P < 0.05$

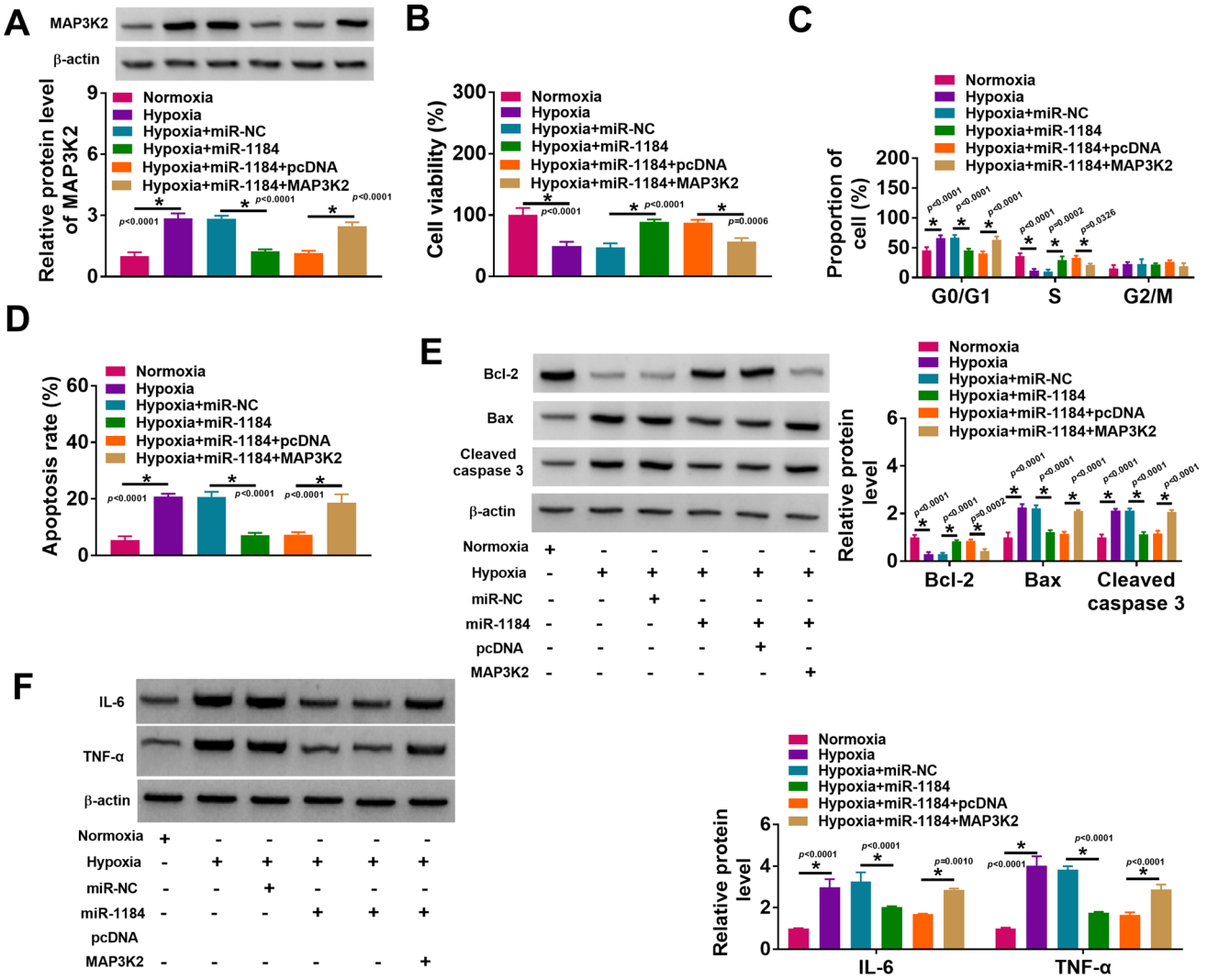
A
MAP3K2
β-actin
Relative protein level of MAP3K2
B
Cell viability (%)
C
Proportion of cell (%)
G0/G1
S
G2/M
D
Apoptosis rate (%)
E
Bcl-2
Bax
Cleaved caspase 3
β-actin
Relative protein level
F
IL-6
TNF-α
β-actin
Normoxia
Hypoxia
miR-NC
miR-1184
pcDNA
MAP3K2
G
IL-6 (pg/mL)
H
TNF-α (pg/mL)
I
Relative MDA level
J
Relative SOD activity
K
Relative glucose uptake
L
Relative lactate production
Normoxia
Hypoxia
Hypoxia+miR-NC
Hypoxia+miR-1184
Hypoxia+miR-1184+pcDNA
Hypoxia+miR-1184+MAP3K2

◂**Fig. 7** MiR-1184 overexpression rescued hypoxia-induced AC16 cell injury by MAP3K2. AC16 cells were treated with normoxia, hypoxia, hypoxia + miR-NC, hypoxia + miR-1184, hypoxia + miR-1184 + pcDNA, or hypoxia + miR-1184 + MAP3K2 expression plasmid. **A** The protein level of MAP3K2 in AC16 cells was measured via western blot. **B** AC16 cell viability was evaluated by CCK-8 assay. **C** and **D** Cell cycle and cell apoptosis in AC16 cells were analyzed by flow cytometry analysis. **E** The protein levels of Bcl-2, Bax, and cleaved caspase 3 in AC16 cells were measured via western blot. **F**–**H** The concentrations of IL-6 and TNF-α in AC16 cells were examined via western blot and ELISA. **I** and **J** MDA level and SOD activity were examined by commercial kits. **K** and **L** The levels of glucose uptake and lactate production in AC16 cells were examined with commercial kits. $^{*}P < 0.05$

MiR-1184 overexpression relieved hypoxia-induced AC16 cell injury by targeting MAP3K2

Furthermore, the effects of miR-1184 and MAP3K2 on hypoxia-induced AC16 cell injury were investigated. As shown in Fig. 7A, miR-1184 overexpression reduced the MAP3K2 protein level in hypoxia-treated AC16 cells, while the transfection of the MAP3K2 overexpression vector reversed the effect. CCK-8 assays revealed that miR-1184 overexpression promoted cell viability of hypoxia-treated AC16 cells, while the effect was weakened by MAP3K2 re-expression (Fig. 7B). Flow cytometry analysis showed that miR-1184 overexpression promoted cell cycle progression and repressed cell apoptosis in hypoxia-treated AC16 cells, whereas MAP3K2 enhancement ameliorated the effects (Fig. 7C and D and Supplementary Fig. 2C). Overexpression of miR-1184 increased Bcl-2 level and decreased Bax and cleaved caspase 3 levels in hypoxia-treated AC16 cells, while MAP3K2 elevation abolished these effects (Fig. 7E). Hypoxia-induced elevation of IL-6 and TNF-α in AC16 cells was reversed by miR-1184 overexpression, but MAP3K2 upregulation alleviated the effects of miR-1184 overexpression (Fig. 7F–H). MiR-1184 overexpression decreased MDA level and promoted SOD activity in hypoxia-treated AC16 cells, whereas the effects were reversed by MAP3K2 re-expression (Fig. 7I and J). Additionally, miR-1184 overexpression increased glucose uptake and lactate production in hypoxia-treated AC16 cells, while MAP3K2 overexpression reversed the effects (Fig. 7K and L). Collectively, miR-1184 overexpression alleviated hypoxia-induced AC16 cell damage by targeting MAP3K2.

Overexpression of MAP3K2 reversed the effect of circHSPG2 knockdown on hypoxia-induced AC16 cell injury

To elucidate whether the protective effect of circHSPG2 knockdown on hypoxia-induced AC16 cell injury was due to MAP3K2 reduction, we elevated MAP3K2 expression with an expression plasmid in circHSPG2-silenced AC16 cells under hypoxia. Transfection of the MAP3K2 expression plasmid significantly reversed si-circHSPG2#1-mediated MAP3K2 reduction in hypoxia-induced AC16 cells (Fig. 8A). Overexpression of MAP3K2 strongly abolished si-circHSPG2#1-mediated cell viability enhancement (Fig. 8B), cell cycle arrest (Fig. 8C), and apoptosis suppression (Fig. 8D and E, and Supplementary Fig. 2D). Moreover, increased MAP3K2 expression reversed si-circHSPG2#1-imposed alteration on IL-6 expression, TNF-α secretion (Fig. 8F–H), MDA level (Fig. 8I), SOD activity (Fig. 8J), glucose uptake level (Fig. 8K), and lactate production (Fig. 8L) in hypoxia-induced AC16 cells. All these findings demonstrated that the protective effect of circHSPG2 knockdown on hypoxia-induced AC16 cell injury was dependent, at least in part, on the MAP3K2 reduction.

Discussion

Despite decades of investigation, effective treatment strategies are still limited in AMI (Sulo et al. 2019). Thus, uncovering the molecular basis of AMI pathogenesis is crucial for the development of new effective treatments. CircRNAs have been identified as vital regulators in AMI development (Yang et al. 2021). Here, we demonstrated that circHSPG2 silencing protected human cardiomyocytes from hypoxia-induced injury by the miR-1184/MAP3K2 axis.

In this study, the hypoxia-induced cardiomyocyte injury model was established by treating AC16 cells with hypoxia. In hypoxia-treated AC16 cells, cell apoptosis, oxidative stress, and inflammation were promoted. A previous study demonstrated that circHSPG2 is overexpressed in AMI patients (Yin et al. 2021). Moreover, loss of circHSPG2 has been shown to relieve cardiomyocyte dysfunction induced by hypoxia (Zhao et al. 2022). Our findings confirmed that circHSPG2 expression was elevated in AMI serum and hypoxia-stimulated AC16 cells. Moreover, circHSPG2 depletion mitigated hypoxia-induced injury in AC16 cells by impacting cell apoptosis, inflammation, and oxidative stress.

Many miRNAs induce the dysfunction of cardiomyocytes during AMI (Ruan et al. 2021; Xiong et al. 2021; Tan et al. 2021). In the current paper, we first showed that circHSPG2 directly targeted miR-1184 and regulated miR-1184 expression. MiR-1184 can inhibit myocardial injury and apoptosis in AMI (Chen et al. 2021). This study also uncovered the involvement of miR-1184 in the regulation of circROBO2 in AMI pathogenesis (Chen et al. 2021). Our study showed the reduction of miR-1184 expression in AMI patients and hypoxia-exposed AC16 cells. Importantly, circHSPG2 knockdown alleviated hypoxia-stimulated AC16 damage by upregulating miR-1184.

MAP3K2, a member of the serine/threonine protein kinase family, is involved in some important biological

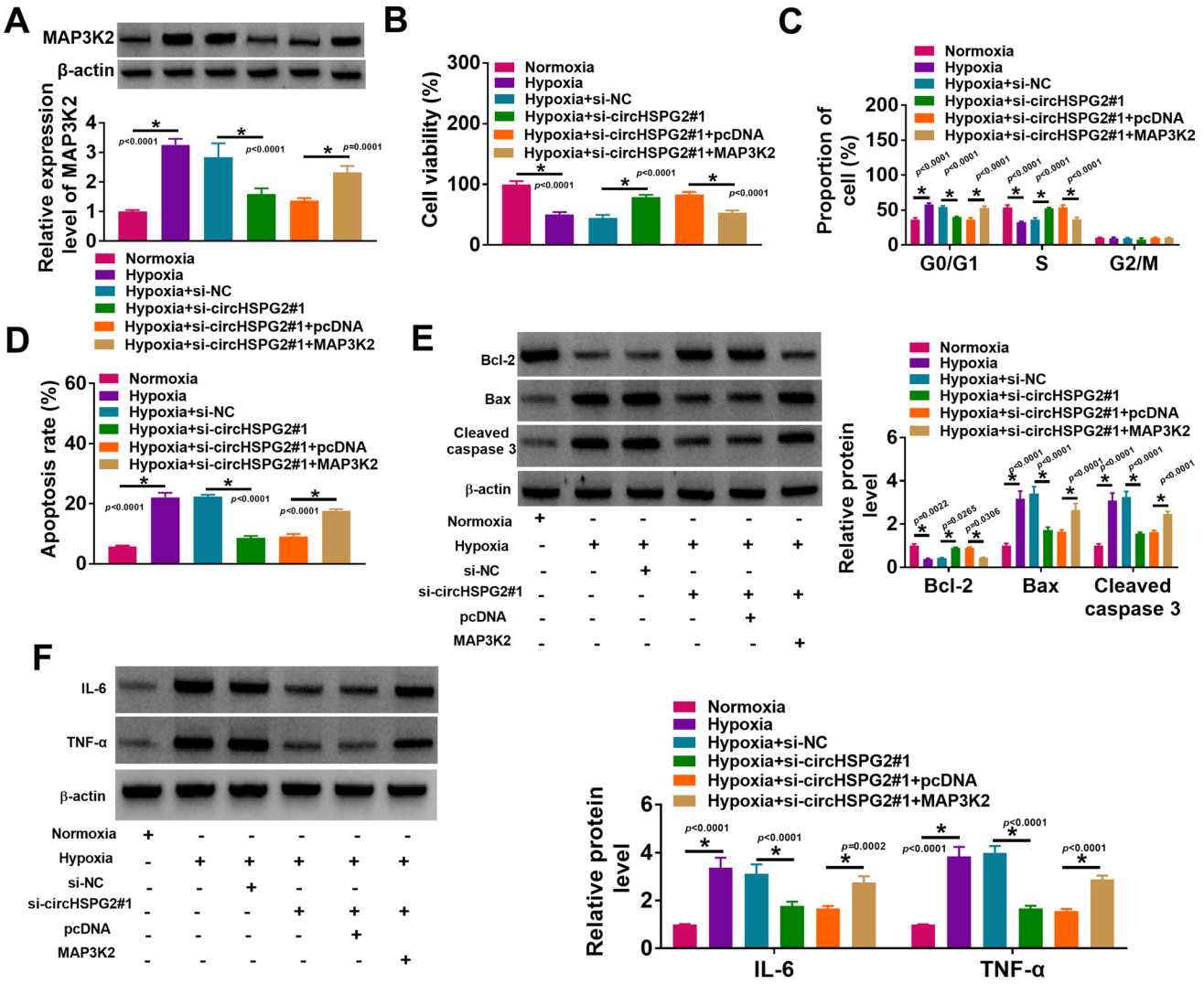
A
MAP3K2
β-actin
Relative expression level of MAP3K2
B
Cell viability (%)
C
Proportion of cell (%)
G0/G1
S
G2/M
D
Apoptosis rate (%)
E
Bcl-2
Bax
Cleaved caspase 3
β-actin
Relative protein level
F
IL-6
TNF-α
β-actin
Normoxia
Hypoxia
Hypoxia+si-NC
Hypoxia+si-circHSPG2#1
Hypoxia+si-circHSPG2#1+pcDNA
Hypoxia+si-circHSPG2#1+MAP3K2
si-NC
si-circHSPG2#1
pcDNA
MAP3K2
G
IL-6 (pg/mL)
H
TNF-α (pg/mL)
I
Relative MDA level
J
Relative SOD activity
K
Relative glucose uptake
L
Relative lactate production

◂**Fig. 8** MiR-1184 overexpression rescued hypoxia-induced AC16 cell injury by MAP3K2. AC16 cells were treated with normoxia, hypoxia, hypoxia + si-NC, hypoxia + si-circHSPG2#1, hypoxia + si-circHSPG2#1 + pcDNA, or hypoxia + si-circHSPG2#1 + MAP3K2 expression plasmid. **A** The protein level of MAP3K2 in AC16 cells was measured via western blot. **B** AC16 cell viability was evaluated by CCK-8 assay. **C** and **D** Cell cycle and cell apoptosis in AC16 cells were analyzed by flow cytometry analysis. **E** The protein levels of Bcl-2, Bax, and cleaved caspase 3 in AC16 cells were measured via western blot. **F**–**H** The concentrations of IL-6 and TNF-α in AC16 cells were examined via western blot and ELISA. **I** and **J** MDA level and SOD activity were examined by commercial kits. **K** and **L** The levels of glucose uptake and lactate production in AC16 cells were examined with commercial kits. $^{*}P < 0.05$

processes (Zhu et al. 2021; Wu et al. 2021). MAP3K2 has been identified as the target of multiple miRNAs, such as miR-335 (Wang and Wen 2020), miR-379-5p (Lv et al. 2019), and miR-582-5p (Wang and Zhang 2018). Here, we verified, for the first time, that MAP3K2 was a miR-1184 target. MiR-338 targets MAP3K2 to restrain cardiomyocyte apoptosis and improve cardiac function in rats with myocardial infarction (Fu et al. 2020). MiR-335 can reduce myocardial inflammation, oxidative stress, and apoptosis in myocardial infarction rats by targeting MAP3K2 (Wang et al. 2021). In the present research, our results demonstrated that miR-1184 repressed cell apoptosis, inflammation, and oxidative stress in the hypoxia-induced AMI cell model through MAP3K2. These findings suggest that the miR-335/MAP3K2, miR-338/MAP3K2, and miR-1184/MAP3K2 axes may be three paralleled or interactional regulatory mechanisms in AMI pathogenesis, which together constitute a complex regulatory network in the regulation of MAP3K2 in AMI. More importantly, we confirmed that circHSPG2 modulated MAP3K2 expression via miR-1184, suggesting the regulation of circHSPG2/miR-1184/MAP3K2 cascade in hypoxia-induced cardiomyocyte injury. Similarly, circHSPG2 has been implicated in hypoxia-induced cardiomyocyte injury through the miR-25-3p/PAWR axis (Zhao et al. 2022). There may be other miRNA/mRNA axes that remain to be elucidated in the regulation of circHSPG2.

Cardiac oxidative stress and inflammation occur during ischemia/reperfusion in AMI and can result in adverse cardiac remodeling and adverse clinical events (Neri et al. 2015; Mahtta et al. 2020). Targeting inflammation and oxidative stress may improve cardiovascular outcomes (Neri et al. 2015). Dysregulation of MAP3K2 is associated with myocardial inflammation and oxidative stress in myocardial infarction rats (Wang et al. 2021). We uncovered, for the first time, that silencing of circHSPG2 relieved hypoxia-induced AC16 cardiomyocyte injury by repressing cell inflammation and oxidative stress through the miR-1184/MAP3K2 axis. Based on these findings, targeting circHSPG2 may provide an opportunity for the development of molecularly targeted therapeutics against AMI. In this study, we used proliferating and immortalized AC16 cells under hypoxia conditions as an in vitro AMI model. In fact, the hypoxia-induced AC16 cells do not exactly mimic terminally differentiated cardiomyocytes under AMI, which is the limitation of this paper. The current study only addresses the immediate cellular effect of hypoxia response.

Taken together, circHSPG2 knockdown mitigated hypoxia-induced AC16 cell injury by regulating the miR-1184/MAP3K2 axis. This study provides a novel insight into AMI pathogenesis and may be helpful for AMI treatment. However, our results still need to be validated by in vivo experiments.

Supplementary Information The online version contains supplementary material available at https://doi.org/10.1007/s12192-023-01328-x.

Acknowledgements Thanks to all participants involved in this study.

Funding This study was supported by the National Natural Science Foundation of China. Grant/Award Numbers: 81400217, 81570345.

Data availability The datasets used and analyzed during the current study are available from the corresponding author on reasonable request.

Declarations

Ethics approval and consent to participate The participants signed written informed consents and the Ethics Committee of the Second Hospital of Hebei Medical University approved the research.

Consent for publication Not applicable.

Conflict of interest The authors declare no competing interests.

References

Boateng S, Sanborn T (2013) Acute myocardial infarction. Dis Mon 59:83–96

Chen TP, Zhang NJ, Wang HJ, Hu SG, Geng X (2021) Knockdown of circROBO2 attenuates acute myocardial infarction through regulating the miR-1184/TRADD axis. Mol Med 27:21

Del Re DP, Amgalan D, Linkermann A, Liu Q, Kitsis RN (2019) Fundamental mechanisms of regulated cell death and implications for heart disease. Physiol Rev 99:1765–1817

Fabian MR, Sonenberg N, Filipowicz W (2010) Regulation of mRNA translation and stability by microRNAs. Annu Rev Biochem 79:351–379

Fu DL, Jiang H, Li CY, Gao T, Liu MR, Li HW (2020) MicroRNA-338 in MSCs-derived exosomes inhibits cardiomyocyte apoptosis in myocardial infarction. Eur Rev Med Pharmacol Sci 24:10107–10117

Gong FF, Vaitenas I, Malaisrie SC, Maganti K (2021) Mechanical complications of acute myocardial infarction: a review. JAMA Cardiol 6:341–349

Ling P, Tang R, Wang H, Deng X, Chen J (2021) miR-1184 regulates inflammatory responses and cell apoptosis by targeting TRADD in an LPS-induced cell model of sepsis. Exp Ther Med 21:630

Liu B, Li J, Cairns MJ (2014) Identifying miRNAs, targets and functions. Brief Bioinform 15:1–19

Lu L, Liu M, Sun R, Zheng Y, Zhang P (2015) Myocardial Infarction: symptoms and Treatments. Cell Biochem Biophys 72:865–867

Lv X, Wang M, Qiang J, Guo S (2019) Circular RNA circ-PITX1 promotes the progression of glioblastoma by acting as a competing endogenous RNA to regulate miR-379-5p/MAP3K2 axis. Eur J Pharmacol 863:172643

Mahtta D, Sudhakar D, Koneru S, Silva GV, Alam M, Virani SS et al (2020) Targeting inflammation after myocardial infarction. Curr Cardiol Rep 22:110

Memczak S, Jens M, Elefsinioti A, Torti F, Krueger J, Rybak A et al (2013) Circular RNAs are a large class of animal RNAs with regulatory potency. Nature 495:333–338

Neri M, Fineschi V, Di Paolo M, Pomara C, Riezzo I, Turillazzi E et al (2015) Cardiac oxidative stress and inflammatory cytokines response after myocardial infarction. Curr Vasc Pharmacol 13:26–36

Panda AC (2018) Circular RNAs act as miRNA sponges. Adv Exp Med Biol 1087:67–79

Ren K, Li B, Jiang L, Liu Z, Wu F, Zhang Y et al (2021) circ_0023461 Silencing protects cardiomyocytes from hypoxia-induced dysfunction through targeting miR-370-3p/PDE4D signaling. Oxid Med Cell Longev 2021:8379962

Ruan Y, Li H, Cao X, Meng S, Jia R, Pu L et al (2021) Inhibition of the lncRNA DANCR attenuates cardiomyocyte injury induced by oxygen-glucose deprivation via the miR-19a-3p/MAPK1 axis. Acta Biochim Biophys Sin (shanghai) 53:1377–1386

Sulo G, Igland J, Sulo E, Overland S, Egeland GM, Vollset SE et al (2019) Mortality following first-time hospitalization with acute myocardial infarction in Norway, 2001–2014: time trends, underlying causes and place of death. Int J Cardiol 294:6–12

Sun JY, Shi Y, Cai XY, Liu J (2020) Potential diagnostic and therapeutic value of circular RNAs in cardiovascular diseases. Cell Signal 71:109604

Tan J, Pan W, Chen H, Du Y, Jiang P, Zeng D et al (2021) Circ_0124644 Serves as a ceRNA for miR-590-3p to promote hypoxia-induced cardiomyocytes injury via regulating SOX4. Front Genet 12:667724

Wang Y, Wen F (2020) MicroRNA-335 inhibits the growth, chemosensitivity, and metastasis of human breast cancer cells by targeting MAP3K2. J BUON 25:666–674

Wang LL, Zhang M (2018) miR-582-5p is a potential prognostic marker in human non-small cell lung cancer and functions as a tumor suppressor by targeting MAP3K2. Eur Rev Med Pharmacol Sci 22:7760–7767

Wang X, Chen Y, Liu W, Liu T, Sun D (2020) Hsa_circ_0128846 promotes tumorigenesis of colorectal cancer by sponging hsa-miR-1184 and releasing AJUBA and inactivating Hippo/YAP signalling. J Cell Mol Med 24:9908–9924

Wang AD, Dai LF, Yang L, Wang YS, Hao XH, Liu ZC et al (2021) Upregulation of miR-335 reduces myocardial injury following myocardial infarction via targeting MAP3K2. Eur Rev Med Pharmacol Sci 25:344–352

Wu N, Chen D, Sun H, Tan J, Zhang Y, Zhang T et al (2021) MAP3K2 augments Th1 cell differentiation via IL-18 to promote T cell-mediated colitis. Sci China Life Sci 64:389–403

Xiong X, Liu J, He Q, Dai R, Zhang H, Cao Z et al (2021) Long non-coding RNA NORAD aggravates acute myocardial infarction by promoting fibrosis and apoptosis via miR-577/COBLL1 axis. Environ Toxicol 36:2256–2265

Yan X, Gan Y, Chen H, Liu G, Hu S, Zhou J (2017) The miRNA expression profile in acute myocardial infarct using sheep model with left ventricular assist device unloading. Biomed Res Int 2017:4352450

Yang D, Qian H, Fang Z, Xu A, Zhao S, Liu B et al (2020) Silencing circular RNA VANGL1 inhibits progression of bladder cancer by regulating miR-1184/IGFBP2 axis. Cancer Med 9:700–710

Yang W, Sun L, Cao X, Li L, Zhang X, Li J et al (2021) Detection of circRNA biomarker for acute myocardial infarction based on system biological analysis of RNA expression. Front Genet 12:686116

Ye L, Chang YH, Xiong Q, Zhang P, Zhang L, Somasundaram P et al (2014) Cardiac repair in a porcine model of acute myocardial infarction with human induced pluripotent stem cell-derived cardiovascular cells. Cell Stem Cell 15:750–761

Yin L, Tang Y, Jiang M (2021) Research on the circular RNA bioinformatics in patients with acute myocardial infarction. J Clin Lab Anal 35:e23621

Zhai C, Qian G, Wu H, Pan H, Xie S, Sun Z et al (2020) Knockdown of circ_0060745 alleviates acute myocardial infarction by suppressing NF-kappaB activation. J Cell Mol Med 24:12401–12410

Zhang Y, Li Z, Wang J, Chen H, He R, Wu H (2022) CircTRRAP Knockdown has cardioprotective function in cardiomyocytes via the signal regulation of miR-370-3p/PAWR axis. Cardiovasc Ther 2022:7125602

Zhao C, Liu J, Ge W, Li Z, Lv M, Feng Y et al (2020) Identification of regulatory circRNAs involved in the pathogenesis of acute myocardial infarction. Front Genet 11:626492

Zhao Y, Wang S, Liu S, Yan Q, Li Y, Liu Y (2022) CircHSPG2 absence weakens hypoxia-induced dysfunction in cardiomyocytes by targeting the miR-25-3p/PAWR axis. Cardiovasc Diagn Ther 12:589–602

Zhu B, Mitheera V, Finch-Edmondson M, Lee Y, Wan Y, Sudol M et al (2021) miR-582-5p is a tumor suppressor microRNA targeting the hippo-YAP/TAZ signaling pathway in Non-Small Cell Lung Cancer. Cancers (Basel) 13:756